[CANCER RESEARCH 59, 1259–1267, March 15, 1999]

Dysregulation of the Cyclin-dependent Kinase Inhibitor p21$^{WAF1/CIP1/MDA6}$ Increases the Susceptibility of Human Leukemia Cells (U937) to 1-β-D-Arabinofuranosylcytosine-mediated Mitochondrial Dysfunction and Apoptosis[1]

Zhiliang Wang, Glenn Van Tuyle, Daniel Conrad, Paul B. Fisher, Paul Dent, and Steven Grant[2]

Departments of Medicine [Z. W., S. G.], Pharmacology [S. G.], Microbiology [D. C., S. G.], Radiation Oncology [P. D.], and Biochemistry [G. V., S. G.], Medical College of Virginia, Virginia Commonwealth University, Richmond, Virginia 23298-0230, and the Departments of Pathology and Urology, Columbia University College of Physicians and Surgeons, New York, New York 10032 [P. B. F.]

ABSTRACT

The effects of dysregulation of the cyclin-dependent kinase inhibitor p21$^{WAF1/CIP1}$ on the apoptotic response of U937 monocytic leukemia cells to 1-β-D-arabinofuranosylcytosine (ara-C) were examined. After a 6-h exposure to 1 μM ara-C, cells stably transfected with a p21$^{WAF1/CIP1}$ antisense construct were significantly more sensitive to the induction of classic apoptotic morphology, DNA fragmentation, caspase-3 activation, poly(ADP-ribose) polymerase degradation, and underphosphorylation of the retinoblastoma protein (pRb) than their empty-vector counterparts. Enhanced susceptibility of antisense-expressing cells to ara-C was accompanied by a corresponding reduction in clonogenic and suspension culture growth. The increased sensitivity of these cells to ara-C-mediated lethality could not be attributed to cytokinetic perturbations, nor did ara-CTP formation or (ara-C)DNA incorporation differ significantly between the cell lines. Moreover, synchronization of p21 antisense-expressing cells in S-phase by aphidicolin block resulted in a further increase in ara-C-mediated apoptosis, suggesting enhanced drug sensitivity of the S-phase cell fraction. After exposure to ara-C, p21 antisense-expressing cells displayed a greater decline in mitochondrial membrane potential ($\Delta\psi_m$) and generation of reactive oxygen species than their empty-vector counterparts, as well as early potentiation (*e.g.*, within 2–4 h) of cytochrome *c* release into the cytosolic S-100 fraction. Lastly, ara-C-mediated increases in mitogen-activated protein kinase activity over basal levels were attenuated in p21 antisense-expressing cells. Collectively, these findings indicate that dysregulation of the cyclin-dependent kinase inhibitor p21$^{WAF1/CIP1}$ increases the susceptibility of U937 human leukemia cells to ara-C-related lethality, and this phenomenon occurs as a relatively early event that is independent of cell cycle or pharmacodynamic factors and is associated with mitochondrial perturbations implicated in activation of the apoptotic protease cascade.

INTRODUCTION

The CDKI[3] p21$^{WAF1/CIP1/MDA6}$ belongs to a group of cell cycle regulatory proteins that includes p27^{KIP1} and p57^{KIP2} (1, 2). These proteins inhibit the activity of cyclin/CDK complexes and consequently play important roles in cell cycle arrest events accompanying DNA damage and cellular maturation (3). p21$^{WAF1/CIP1}$ has been referred to as a universal CDKI in view of its ability to inhibit multiple CDKs, including CDK1 (p34^{cdc2}), CDK2, and CDK4/6 (4). After DNA damage, the p53-dependent induction of p21$^{WAF1/CIP1}$ leads to G_1 arrest, permitting cells to undergo DNA repair, or if the damage is extensive, apoptosis (5). However, p21$^{WAF1/CIP1}$ is also induced in p53-null human leukemia cells exposed to differentiation-inducing agents such as tumor-promoting phorboids (*e.g.*, PMA; 6, 7).

In addition to its role in checkpoint regulation, there is accumulating evidence that p21$^{WAF1/CIP1}$ and other CDKIs may have a significant impact on the response of neoplastic cells to cytotoxic agents. For example, p21$^{WAF1/CIP1}$-deficient colorectal carcinoma cells have been shown to be more sensitive to a variety of DNA-damaging agents and ionizing radiation than their wild-type counterparts, a phenomenon attributed to uncoupling of S-phase and mitosis (8, 9). More recently, inducible expression of p21$^{WAF1/CIP1}$ has been found to reduce the sensitivity of glioblastoma cells to nitrosoureas and cisplatin (10). These findings are compatible with the results of studies demonstrating that other CDKIs, including p27 and p16, decrease the susceptibility of tumor cells to hydroperoxycyclophosphamide- and dexamethasone-mediated apoptosis, respectively (11, 12). Aside from the possibilities that CDKI dysregulation promotes inappropriate cell cycle traverse after cytotoxic drug insult (7) or interferes with DNA repair (13), the mechanism(s) by which CDKIs modulate drug sensitivity remains to be fully elucidated.

The antimetabolite ara-C, a highly active agent used in the treatment of acute leukemia, effectively induces apoptosis in leukemic cells (14). It does not, however, induce p21, at least in cells lacking functional p53 (6). Previously, we described the effects of stable transfection of human HL-60 promyelocytic leukemic cells with a p21$^{WAF1/CIP1}$ antisense construct on responses to the tumor-promoting PMA (15) and have recently extended these findings to the human myelomonocytic leukemic cell line U937 (16). Dysregulation of p21$^{WAF1/CIP1}$ in these cells has a variety of downstream consequences, including impairment in the ability of PMA to inhibit the activity of CDK2, dephosphorylate the retinoblastoma protein (pRb), induce G_1 arrest, and trigger a cellular maturation program (16). Disruption of p21$^{WAF1/CIP1}$ function did not, however, appreciably sensitize HL-60 cells to ara-C-related antiproliferative effects (15). The purpose of the present studies was to characterize the effects of p21$^{WAF1/CIP1}$ dysregulation on the apoptotic response of myelomonocytic leukemia cells to ara-C to identify the factor or factors that might be responsible for alterations in drug sensitivity. Our results indicate that in marked contrast to HL-60 cells, interference with p21$^{WAF1/CIP1}$ induction dramatically increases the susceptibility of U937 cells to ara-C-mediated apoptosis, and that this effect that occurs very early in the course of drug exposure. Furthermore, our results suggest that this phenomenon involves lowering of the threshold for ara-C-induced mitochondrial dysfunction and cytochrome *c* release, events postu-

Received 9/14/98; accepted 1/18/99.

The costs of publication of this article were defrayed in part by the payment of page charges. This article must therefore be hereby marked *advertisement* in accordance with 18 U.S.C. Section 1734 solely to indicate this fact.

[1] This work was supported by awards CA63753, CA72955, CA77141, and CA35675 from the NIH, a Translational Research Award from the Leukemia Society of America (6405-97), the "V" Foundation, and the Chernow Endowment Trust. P. B. F. is the Chernow Research Scientist. Portions of this work were presented in preliminary form at the meeting of the American Association for Cancer Research, New Orleans, LA, March 28-April 1, 1998.

[2] To whom requests for reprints should be addressed, at Medical College of Virginia, MCV Station Box 230, Richmond, VA 23298. Phone: (804) 828-5211; Fax: (804) 828-8079.

[3] The abbreviations used are: CDKI, cyclin-dependent kinase inhibitor; PMA, phorbol-12 myristate-13 acetate; ara-C, 1-β-D-arabinofuranosylcytosine; ara-CTP, 1-β-D-arabinofuranosylcytosine 5′-triphosphate; APH, aphidicolin; PBS-T, PBS-Tween; CDK, cyclin-dependent kinase; PARP, poly(ADP-ribose) polymerase; $DiOC_6$, 3,3′-dihexyloxacarbocyanin iodide; DHR 123, dihydrorhodamine 123; ROS, reactive oxygen species; SAPK, stress-activated protein kinase; JNK, c-Jun NH_2-terminal kinase; MAPK, mitogen-activated protein kinase.

lated to represent critical initiators of the apoptotic protease cascade (17, 18).

MATERIALS AND METHODS

Cells. The myelomonocytic leukemia cell line U937 was derived from a patient with histiocytic lymphoma (19) and was obtained from American Type Culture Collection. Cells were cultured in RPMI 1640 (Life Technologies, Inc., Grand Island, NY) containing 10% FCS and supplemented with penicillin and streptomycin, sodium pyruvate, MEM essential vitamins, and glutamate as described previously (16). Cells were maintained in a 37°C, 5% CO_2, fully humidified incubator and passed twice weekly.

To obtain antisense-expressing lines, cells were transfected by electroporation with either an empty pREP4 vector (Invitrogen, Carlsbad, CA) or a pREP4 vector containing the $p21^{WAF1/CIP1}$ coding region in the antisense orientation, as described previously (15). After selection in hygromycin (Life Technologies, Inc.; 400 μg/ml), individual cells were cloned after limiting dilution. Several clones were then selected that exhibited the greatest attenuation of $p21^{WAF1/CIP1}$ expression when exposed to 10 nM PMA for 24 h. Two such clones, designated U937/p21AS(F4) and U937/p21AS(B8), as well as a clone containing the pREP4 empty vector (U937/pREP4), were used in all subsequent experiments. All experiments were performed using logarithmically growing cells (cell density 3–5 $\times$ 10^5 cells/ml). Cells were tested for *Mycoplasma* contamination using the Gen-Probe kit (Gen-Probe, La Jolla, CA) and found to be negative.

Drugs and Chemicals. ara-C was purchased from Sigma Chemical Co. (St. Louis, MO) and maintained as a dry power at −20 C. It was reformulated in PBS before use. ara-CTP was purchased from Sigma, stored desiccated at −20°C, and formulated in water before use. PMA and APH were also purchased from Sigma, diluted in DMSO, and stored frozen under light-protected conditions at −20°C before use. In no case did the final DMSO concentration exceed 0.1%, nor did vehicle controls alter apoptotic or differentiation responses. 5-[^{3}H]ara-C (24 Ci/mmol) was purchased from Amersham Radiochemicals (Arlington, IL). $DiOC_6$, carbamoyl cyanide *m*-chlorophenylhydrazone, and DHR 123 were purchased from Molecular Probes (Eugene, OR).

Assessment of Apoptosis. Apoptotic cells were evaluated by morphological criteria as reported previously (20). After treatment of cells, cytospin preparations of the cell suspensions were fixed and stained with Wright-Giemsa. Cell morphology was evaluated by light microscopy, and apoptotic cells were identified by the the appearance of cell shrinkage, nuclear condensation, and/or the appearance of membrane-bound apoptotic bodies. Five to seven randomly selected fields were evaluated for each condition, encompassing a total of at least 500 cells. Alternatively, the appearance of oligonucleosomal DNA fragmentation characteristic of apoptosis was determined by agarose gel electrophoresis as described earlier (20). After drug exposure, pelleted cells (2 $\times$ 10^7 cells/condition) were lysed in 0.1% NP40, 10 mM Tris-HCl, and 25 mM EDTA (pH 7.4) containing 200 μg/ml Proteinase K and incubated for 24 h at 56°C. The lysates were then centrifuged at 48,000 $\times$ *g* for 45 min, and the supernatant was adjusted to 200 μg/ml RNase A for 4 h at 37°C. DNA unassociated with intact chromatin residing in the supernatant was then resolved by agarose gel electrophoresis at 6 V/cm in 1$\times$ TBE buffer (Tris-borate/EDTA) for 3 h on 1.8% agarose gels impregnated with ethidium bromide. Each lane was loaded with a volume of cell lysate corresponding to 2 $\times$ 10^6 cells, rather than with a fixed quantity of DNA. To permit estimation of fragment size, 100-bp DNA reference preparations were run in parallel.

Cell Viability. Logarithmically growing U937/pREP4 and p21AS cells were exposed to ara-C for 6 h, washed thoroughly in drug-free medium, and incubated for an additional 24 h in fresh medium. At the end of this time, the cells were enumerated by hemocytometer, and the number of viable cells was determined based upon their exclusion of 0.4% trypan blue dye.

Clonogenic Assay. After drug treatment, cells were enumerated using a hemacytometer, washed free of drug (three times) in 1$\times$ fetal bovine serum-free media, and plated in triplicate in 12-well plates (Costar) containing 500 cells/well, 1 ml of media, 20% fetal bovine serum, and 0.3% Bacto agar (Difco, Detroit, MI; 20). Plates were incubated in a fully humidified atmosphere of 95% air and 5% CO_2 at 37°C, and colonies, consisting of groups of $\geq$50 cells, were scored 10–12 days after plating.

Western Blot Analysis. Equal amounts of protein (25 μg) were separated by SDS-PAGE [5% stacker and 6% (PARP and pRb) or 12% (p21, bcl-2, bcl-xl, bax, and CPP32) or 15% (cytochrome *c*)] and electroblotted onto nitrocellulose as described previously (15). The blots were then blocked in PBS-T (0.05%) and 5% milk for 1 h with the appropriate dilution of primary antibody: PARP (1:10000; Biomol Research Laboratories, Plymouth Meeting, PA); pRb (1:2000; PharMingen, San Diego, CA); bcl-2 (1:2000; Dako, Copenhagen, Denmark); bcl-x_L (1:1000; Santa Cruz Biotechnology, Inc., Santa Cruz, CA); bax (1:2000; Santa Cruz Biotechnology); p21cip1 (1:500; Transduction Laboratories, Lexington, KY); CPP32 (1:2000; Transduction Laboratories); cytochrome *c* (1:2000; PharMingen); c-Myc (provided by Dr. John Cleveland, St. Jude Children's Research Hospital, Memphis, TN; 1:2000); and actin (1:2000; Sigma). A murine IgG1 antibody (G99–549) that primarily reacts with underphosphorylated pRb species was obtained from PharMingen and used at a concentration of 1:2000. Blots were washed two times for 10 min in PBS-T and then incubated with a 1:2000 dilution of peroxidase-conjugated secondary antibodies (Kirkegaard and Perry Laboratories, Inc., Gaithersburg, MD) in PBS-T for 1 h at 22°C. Blots were again washed two times for 10 min in PBS-T and then developed by enhanced chemiluminescence (Pierce).

Preparation of S-100 Fractions and Assessment of Cytochrome *c* Release. U937 cells expressing antisense $p21^{WAF1/CIP1}$ and empty vector-containing controls were harvested after drug treatment by centrifugation at 600 $\times$ *g* for 10 min at 4°C. The cytosolic S-100 fraction was prepared as described (18), with minor modifications. Cell pellets were washed once with ice-cold PBS and resuspended in five volumes of buffer A [20 mM HEPES-KOH (pH 7.5), 10 mM KCl, 1.5 mM $MgCl_2$, 1 mM sodium EDTA, 1 mM sodium EGTA, 1 mM DTT, 0.1 mM phenylmethylsulfonyl fluoride, and 250 mM sucrose]. After being chilled for 30 min on ice, the cells were disrupted by 15 strokes of a glass homogenizer. The homogenate was centrifuged twice to remove unbroken cells and nuclei (750 $\times$ *g*, 10 min, 4°C). S-100 fractions (supernatants) were then obtained by centrifugation at 100,000 $\times$ *g*, 60 min at 4°C. All steps were performed on ice or 4°C. Cytochrome *c* release into the S-100 fraction for each condition was assessed by Western blot analysis of the resulting fractions as detailed above.

Cell Cycle Analysis. After drug treatment, cells were pelleted at 500 $\times$ *g* and resuspended in 70% ethanol. The cells were incubated on ice for at least 1 h and resuspended in 1 ml of cell cycle buffer (0.38 mM sodium citrate, 0.5 mg/ml RNase A, and 0.01 mg/ml propidium iodide) at a concentration of 10 $\times$ 10^5 cells/ml. Samples were stored in the dark at 4°C until analysis (usually within 24 h), using a Becton Dickinson FACScan flow cytometer and ModFit LT 2.0 software (Verity Software, Topsham, ME).

Cell Cycle Synchronization. Synchronization of cells within G_1-S phase of the cell cycle was achieved using an APH block. Cells were treated with 0.15 μg/ml for 24 h and washed in drug-free medium three times before resuspension. Synchronization was confirmed by propidium iodide staining and flow cytometry (see above). Cell viability immediately after release from APH block was routinely >90%, and the percentage of cells in G_1-S at this interval was consistently 85–90%. Moreover, this concentration of APH was found to be without discernible biological effect in U937 cells. Synchronized cells were used for experimentation immediately to prevent cells from reentering the cell cycle.

ara-CTP Formation. Logarithmically growing $p21^{WAF1/CIP1}$ antisense-expressing cells and cells containing the empty vector were exposed to 1 μM ara-C for 6 h, centrifuged for 10 min at 400 $\times$ *g* at 4°C, and washed twice with PBS, and the pellet precipitated with trichloroacetic acid as reported previously (21). Neutralized acid-soluble material was extracted using freon-octylamine, treated with sodium periodate to eliminate ribonucleotides, and subjected to high-pressure liquid chromatographic analysis using a Bio-Rad Model 700 Workstation, a Beckman Medel 260 detector, a Waters Partisil SAX column, and a K_2HPO_4 gradient elution system. Peaks coeluting with authentic ara-CTP standards were integrated automatically and expressed as pmol ara-CTP/10^6 cells.

ara-C(DNA) Incorporation. Assessment of incorporation of ara-C residues into the DNA of U937/p21 antisense-expressing and empty vector control cells was performed using a method described previously (21). After incubation of cells with 1 μM 5-[^{3}H]ara-C for 6 h, cells were pelleted and lysed, and DNA was isolated by phenol-chloroform extraction and ethanol precipitation. DNA was then resuspended in TE buffer, quantitated spectrofluorometrically, and aliquots were added to an aqueous scintillation cocktail before scintillation counting. Values are expressed as pmol 5-[^{3}H]ara-C incorporated/ng DNA.

Assessment of Mitochrondrial Membrane Potential ($\Delta\Psi_m$) and ROS. Mitochrondrial membrane potential was monitored using $DiOC_6$ (17). In addition, DHR 123 was used to measure ROS (22). In the presence of ROS, DHR 123 is oxidized to the highly fluorescent rhodamine 123. For each condition, 4×10^5 cells were incubated for 15 min at 37°C in 1 ml of 40 nM $DiOC_6$ (3) or 1 μM of DHR123 and subsequently analyzed using a Becton Dickinson FACScan cytofluorometer with excitation and emission settings of 488 and 525 nm, respectively. Control experiments documenting the loss of $\Delta\Psi_m$ and generation of ROS were performed by exposing cells to 5 μM carbamoyl cyanide *m*-chlorophenylhydrazone (15 min, 37°C), an uncoupling agent that abolishes the mitochondrial membrane potential, or 10 nM H_2O_2, respectively. Control gates were set as shown in the figures, and loss of $\Delta\psi_m$ or generation of ROS was quantified using the Cyclops program (Cytomation, Boulder, CO).

Determination of SAPK (JNK) and MAPK Activities. A method described previously was used (23). Pelleted cells were washed in PBS, repelleted, and flash-frozen. Cell pellets were lysed in the 25 mM sodium β-glycerophosphate (pH 7.4), containing 5 mM EGTA, 5 mM EDTA, protease inhibitors (5 mM benzamidine, 1 mM phenylmethysulfonyl fluoride, 1 mg/ml soybean trypsin inhibitor, 40 μg/ml pepstatin, 40 μg/ml chymotrypsinogen, 40 μg/ml E64, 40 μg/ml aprotinin, and 1 μM microcystin LR), phosphatase inhibitors (1.0 mM trisodium orthovanadate and 1.0 mM tetrasodium PP_i), 0.05% (w/v) sodium deoxycholate, 1% (v/v) Triton X-100, and 0.1% (v/v) 2-mercaptoethanol. Lysates were clarified by centrifugation at 5000 $\times$ *g* at 4°C for 5 min. SAPK/MAPK was immunoprecipitated from clarified lysates with protein A/agarose-conjugated antibody/antisera. JNK activity was then assayed after immunoprecipitation of p54-JNK1/p46-JNK2 using glutathione-*S*-transferase/c-Jun 1–169 as substrate. Alternatively, MAPK activity was assayed after immunoprecipitation of p42-ERK1/p44-ERK2 using myelin basic protein as substrate. Preimmune controls were also run to ensure selectivity of substate phosphorylation. Reaction mixtures consisted of immunoprecipitated enzyme, substrate, and 0.1 mM [γ-^{32}P]ATP(5000 Ci/pmol) in 25 mM sodium β-glycerophosphate (pH 7.4), containing 15 mM $MgCl_2$, 100 μM trisodium orthovanadate, 0.01% (v/v) 2-β-mercaptoethanol, and 1 μM microcystin LR. Reactions were initiated by the addition of substrate. MAPK reactions were terminated by transfer to p81 filter paper; the filters were rinsed repeatedly in 185 mM orthophosphoric acid and then dehydrated in acetone. JNK assays were terminated by transfer to 10% polyacrylamide gels; phosphorylated products were resolved by electrophoresis, and appropriate substrate bands were excised. Total radioactivity in gels and filters was determined by liquid scintillometry.

Statistical Analysis. The significance of differences between experimental conditions was determined using Student's *t* test for unpaired observations.

RESULTS

In initial studies, the dose-response of empty vector and p21 antisense-expressing cell lines to ara-C-mediated apoptosis was examined (Fig. 1). After a 6-h incubation with increasing concentrations of ara-C, empty vector transfectants (pREP4) displayed a progressive increase in the percentage of cells displaying the characteristic morphological features of apoptosis, reaching a maximum of ~30% at 100 μM (Fig. 1*A*). This response was similar to that observed in untransfected cells (not shown). Both antisense-expressing cell lines (p21AS/F4 and/B8) exhibited a significantly greater susceptibility to apoptosis at each ara-C concentration evaluated. Gel electrophoretic analysis of DNA obtained from cells treated with various concentrations of ara-C also revealed more intensely staining oligonucleosomal bands in p21AS/F4 cells compared with empty vector controls (Fig. 1*B*). In addition, degradation of the M_r 115,000 caspase-3 substrate PARP into its M_r 85,000 cleavage product was considerably more prominent in p21AS/F4 and/B8 cells than in their empty vector counterparts (Fig. 1*C*). As reported previously in the case of p21 antisense-expressing HL-60 cells (15), a 6-h exposure to ara-C did not result in a discernible increase in $p21^{WAF1/CIP1}$ expression (Fig. 1*D*). Taken together, these findings demonstrate that the presence of the p21 antisense construct rendered U937 leukemic cells more sensitive to ara-C-mediated apoptosis.

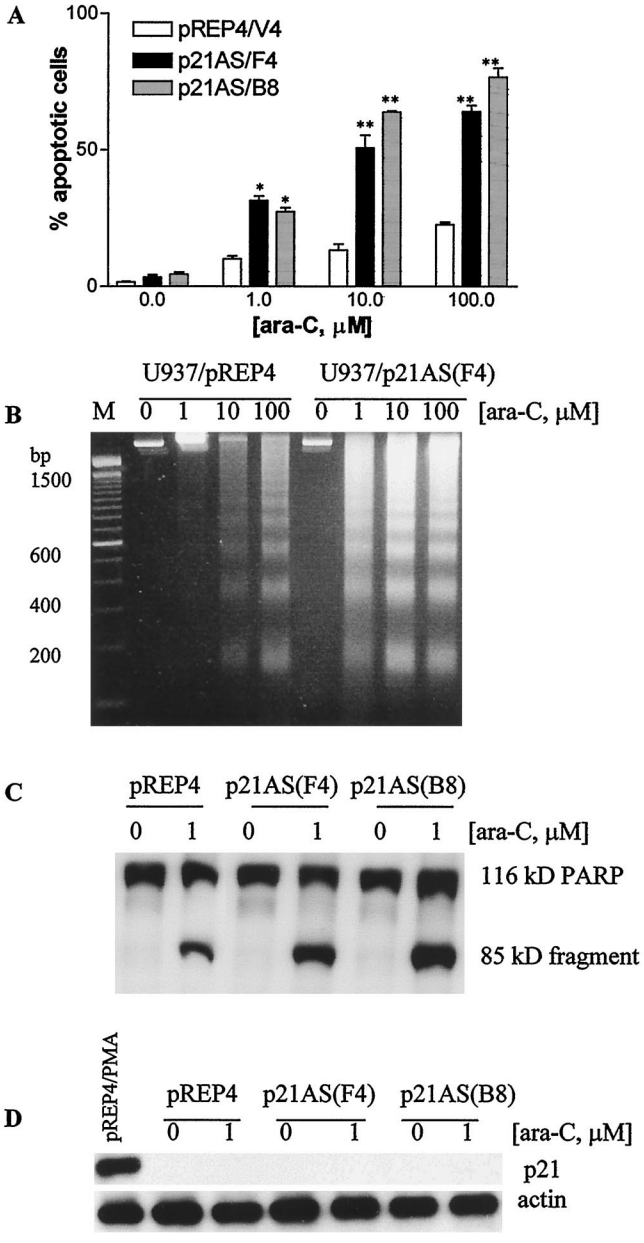

Fig. 1. *A*, cells containing an empty vector (pREP/V4) and two antisense-expressing clones (p21AS/F4 and B8) were exposed to the designated concentration of ara-C for 6 h, after which the percentage of apoptotic cells was determined by evaluating Wright Geimsa-stained specimens as described in the text. Values represent the means for three separate experiments; *bars*, $\pm$1 SD. *, greater than values for empty vector controls; $P \leq 0.05$; **, $P \leq 0.02$. *B*, DNA was extracted from empty vector control and antisense-expressing cells (AS/F4) after a 6-h exposure to the designated concentration of ara-C, subjected to agarose gel electrophoresis, and stained with propidium iodide to visualize internucleosomal DNA cleavage patterns. A standard DNA ladder is shown in the left lane. *C*, after exposure to 1 μM ara-C for 6 h, cells were lysed, protein was extracted, and expression of PARP (20 μg/condition) was assessed by Western analysis as described in the text. Proteolysis of native M_r 116,000 PARP to its M_r 85,000 cleavage product characteristically occurs in cells undergoing apoptosis. *D*, Western analysis of $p21^{WAF1/CIP1}$ expression after exposure of cells to 1 μM ara-C for 6 h. An extract from pREP4 cells treated with 10 nM PMA for 24 h was used as a positive control.

Because the susceptibility of neoplastic cells to diverse chemotherapeutic agents can depend upon the relative abundance of pro- and antiapoptotic members of the Bcl-2 family (24), Western blot analysis was performed to determine if such factors might be responsible for the preceding observations. However, levels of Bcl-2, Bcl-x_L, and Bax

were equivalent in untransfected cells, cells transfected with the empty vector, and in the two p21 antisense-expressing cell lines (data not shown). Furthermore, treatment with 1 μM ara-C for 6 h failed to modify expression of these proteins, rendering it unlikely that alterations in levels of Bcl-2, Bcl-x_L, or Bax could account for the increased sensitivity of the p21antisense-expressing lines to ara-C-induced apoptosis. The cytotoxic actions of ara-C have also been related to formation of its lethal triphosphate derivative, ara-CTP, and/or to incorporation of ara-C residues into elongating DNA strands (25). However, after a 6-h exposure to 1 μM ara-C, both ara-CTP formation (27.6 $\pm$ 3.5 *versus* 31.3 $\pm$ 3.3 pmol ara-CTP/10^6 cells) and ara-C(DNA) incorporation (1.21 $\pm$ 0.23 *versus* 1.51 $\pm$ 0.41 pmol/ng DNA) were equivalent in the pREP4 and p21AS/F4 cell lines ($P \leq 0.05$ in each case; data not shown).

It remained possible that the increased susceptibility of p21 antisense-expressing cells to ara-C might stem from cytokinetic or pharmacodynamic factors. For example, because ara-C is an S-phase-specific agent (26), an increase in the S-phase fraction would render cells more vulnerable to this agent. However, flow cytometric analysis revealed that the S-phase percentage of the pREP4 and p21AS/F4 lines were identical (*e.g.*, 38.6 $\pm$ 3.6 *versus* 40.8 $\pm$ 4.2; $P \geq 0.05$; Fig. 2*A*). Moreover, the sub-G_1 population, corresponding to hypodiploid, apoptotic cells, was clearly greater in p21 antisense-expressing cells after ara-C administration (Fig. 2*B*). Furthermore, the increase in the subdiploid population was observed over a wide range of ara-C concentrations (Fig. 2*C*). Together, these and the preceding findings indicated that the increased susceptibility of p21 antisense-expressing cells to ara-C-mediated apoptosis could not simply be attributed to conventional cytokinetic or pharmacodynamic factors.

It has been shown previously that ara-C-induced apoptosis in human leukemia cells (HL-60) is accompanied by dephosphorylation of the retinoblastoma protein (27). To assess the impact of $p21^{WAF1/CIP1}$ dysregulation on this phenomenon, pRb phosphorylation status was monitored in U937pREP4 and U937p21AS/F4 cells after a 6-h exposure to 1 μM ara-C (Fig. 3). U937/pREP4 cells displayed a marginal increase in abundance of the higher mobility pRb species after treatment with 1 μM ara-C for 6 h (Fig. 3*A*). However, this shift was considerably more pronounced in the U937/p21AS/F4 line, a finding that is distinctly different from that observed previously in p21 antisense-expressing cells treated with PMA (16). Results obtained using the G99-549 murine antibody, which primarily recognizes underphosphorylated pRb (28), supported the notion that $p21^{WAF1/CIP1}$ dysregulation promotes ara-C-mediated pRb dephosphorylation (Fig. 3*B*). In contrast to these findings, expression of c-Myc protein was unperturbed by ara-C treatment in both the p21 antisense-expressing and empty vector control cell lines (Fig. 3*A*).

It is now recognized that a discordance may exist between the appearance of the classic morphological and biochemical features of apoptosis and loss of cellular clonogenic potential (29, 30). To assess the biological consequences of $p21^{WAF1/CIP1}$ dysregulation, the viability of ara-C-treated empty vector and p21 antisense-expressing cells was compared using trypan blue exclusion and clonogenic assays (Fig. 4). After a 6-h exposure to various concentrations of ara-C, p21 antisense-expressing cells displayed a highly significant reduction in the number of viable cells at 24 h (Fig. 4*A*) and in the number of day 12 colonies (Fig. 4*B*) than their empty vector-containing counterparts. These results indicate that the increased susceptibility of p21 antisense-expressing U937cells to ara-C-mediated apoptosis is accompanied by a corresponding loss of leukemic self-renewal capacity.

Subsequent studies were undertaken to elucidate cytokinetic factors potentially involved in the increased sensitivity of p21 antisense-expressing cells. The nucleoside APH, like ara-C, is an inhibitor of DNA polymerase, but unlike ara-C, is not incorporated into elongating DNA strands (31). Although APH is known to induce apoptosis by itself (29), a minimally toxic concentration (0.1 μM) was identified that was capable of arresting ~85% of cells in S-phase after a 24-h exposure (data not shown). Cells were then washed free of APH, and the partially synchronized population was exposed to ara-C as described above. It can be seen from the data shown in Fig. 5 that pretreatment of U937/pREP4 cells with a subtoxic concentration of APH significantly increased the extent of apoptosis resulting from a

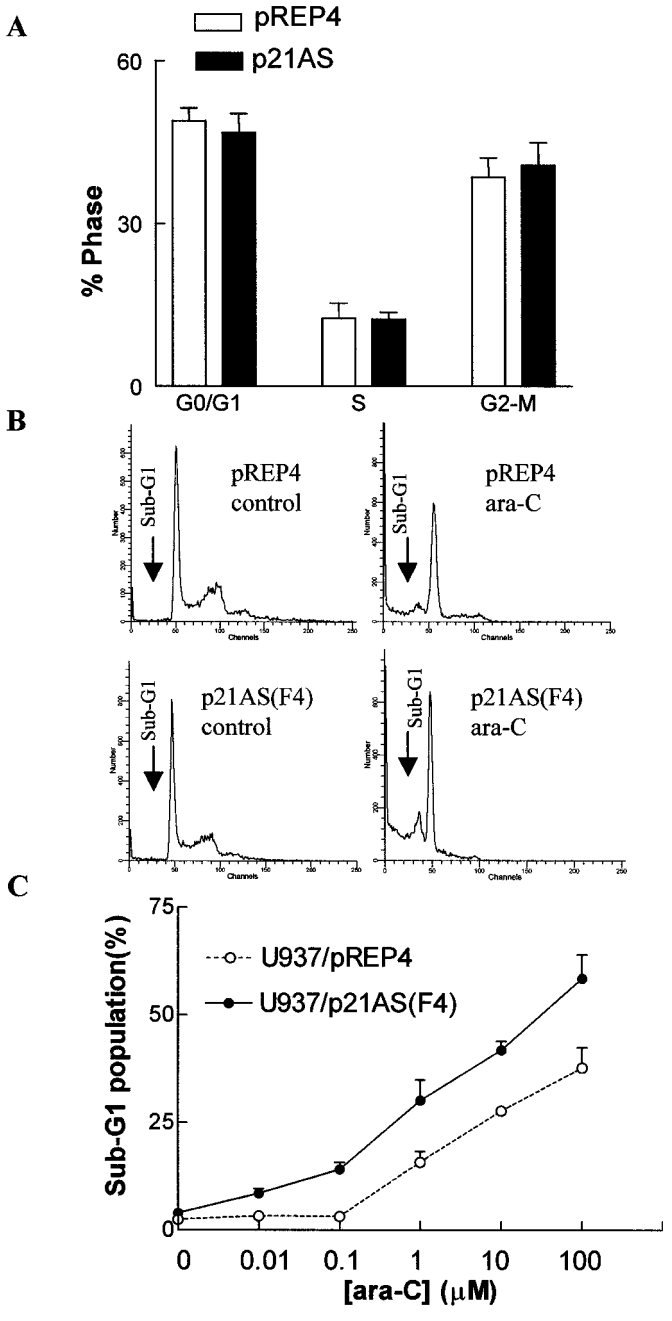

Fig. 2. *A*, cells were incubated with propidium iodide, and cell cycle characteristics were determined using a Becton Dickinson FACScan flow cytometer and ModFit software as described in "Materials and Methods." The percentage of cells in the G_0/G_1, S, and G_2-M fractions of the cell cycle represent the means for three separate experiments; *bars*, SD. *B*, after exposure to 1 μM ara-C for 6 h, cell pellets were incubated in 70% ethanol overnight at 4°C to promote loss of fragmented DNA. The cells were then treated with propidium iodide and subjected to cell cycle analysis as above. The sub-G_1 populations, corresponding to hypodiploid, apoptotic cells, are shown under the *arrows*. *C*, pREP4 and p21AS/F4 cells were exposed to the designated concentration of ara-C for 6 h, after which the sub-G_1 fraction was quantified by flow cytometry as above. Values represent the means for three separate experiments; *bars*, SD.

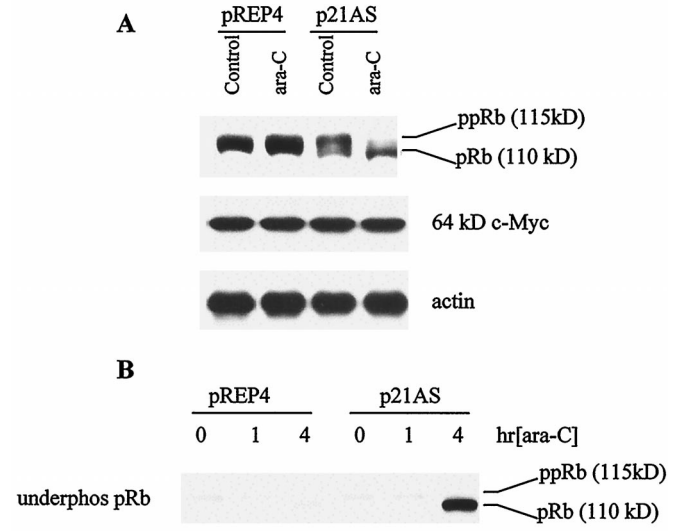

Fig. 3. *A*, pREP4 and p21AS/F4 cells were exposed to 1 μM ara-C for 6 h, after which they were lysed, and expression of pRb and c-Myc were determined by Western blot analysis as described in the text. Each lane was loaded with 10 μg of protein. Phosphorylated pRb characteristically displays a mobility of M_r 116,000, whereas dephosphorylated pRb migrates at M_r 110,000. *B*, cell lysates were obtained and analyzed as above, except that they were probed with a murine antibody that primarily recognizes underphosphorylated pRb (G99-549), as described in the text. The results of a representative study are shown; two additional experiments yielded similar results.

6-h exposure to 1 μM ara-C (Fig. 5*A*). However, a similar effect was observed in U937p21AS/F4 cells; in fact, synchronization with APH permitted this ara-C exposure to induce apoptosis in ~70% of cells (*versus* ~35% in their unsynchronized counterparts). These findings were confirmed by studies examining ara-C-mediated activation of caspase-3 (CPP32; Yama), manifested by the appearance of the M_r 17,000 cleavage product, in cells synchronized by APH pretreatment (Fig. 5*B*). The results of these studies demonstrated that cells synchronized by APH treatment (Fig. 5*B*, *Lanes 4 and 8*) displayed greater caspase-3 cleavage than their unsynchronized counterparts (Fig. 5*B*, *Lanes 3 and 7*); moreover, in each case, caspase -3 cleavage was greater in antisense-expressing (Fig. 5*B*, *Lanes 7 and 8*) than in empty vector-containing cells (Fig. 5*B*, *Lanes 3 and 4*). Taken together, such findings suggest that loss of $p21^{WAF1/CIP1}$ function specifically increases the susceptibility of S-phase cells to ara-C-related cell death, presumably by facilitating activation of the apoptotic caspase cascade.

There is abundant evidence that mitochondrial dysfunction plays an important, and perhaps central, role in apoptotic events (17). To determine what effect $p21^{WAF1/CIP1}$ dysregulation might have on mitochrondrial perturbations accompanying (or responsible for) apoptosis, uptake of the lipophilic fluorochrome $DiOC_6$ was monitored (Fig. 6*A*). Loss of mitochondrial membrane potential ($\Delta\psi_m$) is characteristically associated with reduced cellular accumulation of $DiOC_6$ (17). After a 6-h exposure to 1 μM ara-C, a significantly greater percentage of p21 antisense-expressing cells displayed a reduction in $\Delta\psi_m$ compared with their empty vector counterparts (*e.g.*, 52.8 $\pm$ 3.0% *versus* 30.2 $\pm$ 2.8%; $P \leq 0.02$; $n = 3$). Equivalent results were obtained using the fluorochrome JC-1 (data not shown). Similarly, the generation of ROS by ara-C, manifested by increased staining with DHR 123, was greater in antisense-expressing than in empty vector-containing cells (*e.g.*, 18.7 $\pm$ 1.5% *versus* 5.5 $\pm$ 1.7%; $P \leq 0.02$; $n = 3$; Fig. 6*B*). However, the percentage of cells positive for ROS was less than the percentage of cells displaying loss of $\Delta\psi_m$ (or characteristic apoptotic morphology), suggesting that ROS generation represents a secondary event in this setting. Lastly, ara-C-mediated increases in release of cytochrome *c* into the cytosolic S-100 fraction were enhanced in p21 antisense-expressing cells (relative to empty-vector controls) as early as 2 h after drug exposure and was quite marked at 4–6 h (Fig. 6*C*). Collectively, these findings indicate that $p21^{WAF1/CIP1}$ dysregulation is accompanied by potentiation of mitochondrial dysfunction in ara-C-treated cells, and that this phenomenon represents an early event in the cell death program.

Finally, it has been shown that cellular susceptibility to apoptosis may depend upon the balance between pro- (*e.g.*, JNK/SAPK) *versus* anti- (*e.g.*, ERK/MAPK) apoptotic signaling pathways (32). Furthermore, links between $p21^{WAF1/CIP1}$ and these pathways have been identified, inasmuch as MAP kinase has been shown to be involved in regulation of $p21^{WAF1/CIP1}$ expression (33), and p21 has been reported to inhibit JNK activation (34). Consequently, the effect of $p21^{WAF1/CIP1}$ dysregulation was examined with respect to its effects on ara-C-mediated MAP kinase and JNK activation. Basal JNK activity was equivalent in empty vector controls and the two antisense-expressing lines (*e.g.*, 3.7 $\pm$ 1.2, 3.5 $\pm$ 1.0, and 3.1 $\pm$ 0.6 fmol/min/mg protein; data not shown). In addition, no differences in JNK activation were observed between the cell lines after ara-C exposure. In contrast to these findings, basal MAP kinase activity was significantly higher in p21 AS-expressing cells than in empty vector controls (*e.g.*, 286 $\pm$ 71 and 373 $\pm$ 112 *versus* 103 $\pm$ 26 fmol/min/mg for p21AS/F4, p21AS/B8, and pREP4, respectively; $P \leq 0.05$ in each case; Fig. 7*A*). Furthermore, upon ara-C exposure, pREP4 cells displayed increases

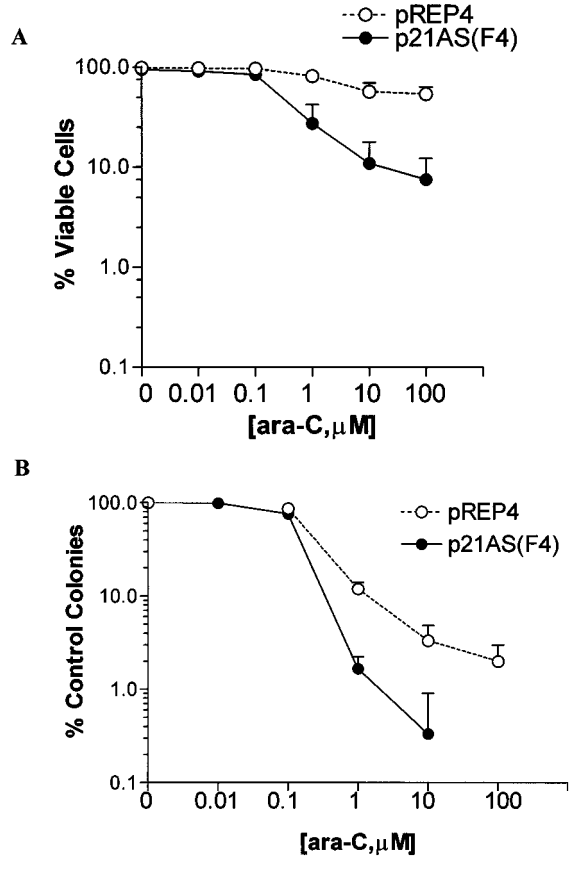

Fig. 4. *A*, pREP4 and p21AS/F4 cells were exposed to the designated concentration of ara-C for 6 h, washed, and resuspended in drug-free medium for an additional 24 h. The percentage of viable cells (relative to untreated controls) was determined by monitoring trypan blue exclusion as described in the text. Values represent the means for three separate experiments; *bars*, SD. *B*, cells were exposed to the designated concentration for 6 h, washed free of drug, and plated in soft agar as described in "Materials and Methods." Colonies, consisting of groups of $\geq$50 cells, were scored on day 12. Values are expressed as the percentage of colonies formed relative to untreated controls and represent the means for three separate experiments; *bars*, SD.

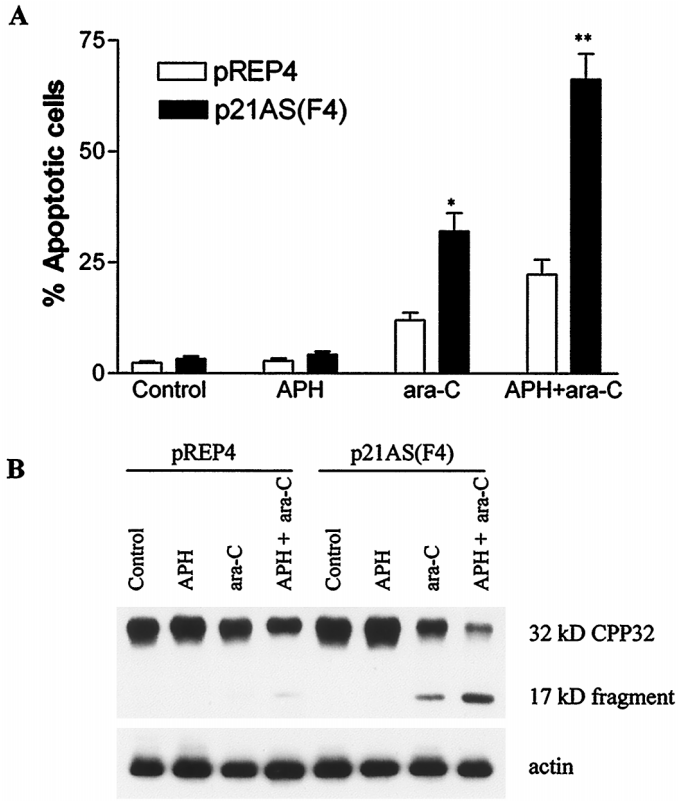

Fig. 5. *A*, pREP4 and p21AS/F4 cells were incubated for 24 h with 0.125 μM APH, after which they were washed free of drug and resuspended in complete medium. After such treatment, 75–85% of the cells accumulated in S-phase. The cells were then exposed to 1 μM ara-C for 6 h, after which the percentage of apoptotic cells was determined by examining Wright Giemsa-stained preparations. Values represent the means for three separate experiments; *bars*, SD. *, significantly greater than values for pREP4 cells; $P \leq 0.02$; **, $P \leq 0.005$. *B*, after treatment as above, expression of the M_r 32,000 Yama protein and its M_r 17,000 cleavage product were monitored by Western blot analysis as described in "Materials and Methods." Each lane was loaded with 10 μg of protein. *Lanes 1–4*, pREP4 cells; *Lanes 5–8*, p21AS/F4 cells. *Lanes 1* and *5*, controls; *Lanes 2* and *6*, APH (0.125 μM; 24 h); *Lanes 3* and *7*, ara-C (1 μM; 6 h); *Lanes 4* and *8*, APH → ara-C. Two additional studies yielded equivalent results.

in MAP kinase activity after 3–4 h, followed by a return toward basal levels (Fig. 7*A*). In contrast, antisense-expressing cells expressed a rapid (*e.g.*, within 15 min) reduction in MAP kinase activity, followed by a partial recovery and subsequent decline (Fig. 7*A*). At no time did antisense-expressing cells exhibit an increase in MAP kinase activity over basal levels. Changes in MAP kinase activity (relative to initial values) are shown more clearly in Fig. 7*B*. However, because basal MAP kinase activity in pREP4 cells was significantly less than that observed in the antisense-expressing lines, absolute levels of activity in the former cells were only slightly greater than (or equivalent to) those detected in the p21AS/F4 and B8 cells 4–6 h after ara-C exposure. Finally, treatment with 100 nM PMA increased MAP kinase activity (at 20 min) by ≥100% in each of the cell lines (data not shown), indicating that constitutive activity was not maximally stimulated in antisense-expressing cells. These findings raise the possibility that the failure of ara-C to activate the cytoprotective MAP kinase signaling pathway over basal levels in $p21^{WAF1/CIP1}$ antisense-expressing cells may contribute to their increased susceptibility to ara-C-mediated apoptosis.

DISCUSSION

The CDKI $p21^{WAF1/CIP1}$, a downstream target of p53, has been implicated in the G_1 arrest response to both DNA-damaging and differentiation-inducing agents (5, 6, 35). Furthermore, evidence that induction of $p21^{WAF1/CIP1}$ in differentiating myocytes is associated with a reduced susceptibility to cell death (36) argues for an antiapoptotic role for this CDKI. Moreover, human colon tumor cells (HCT116) deficient in $p21^{WAF1/CIP1}$ undergo apoptosis more readily than their wild-type counterparts in response to agents such as doxorubicin and ionizing radiation, a phenomenon attributed to uncoupling of S-phase and mitosis (8, 13). More recently, inducible up-regulation of $p21^{WAF1/CIP1}$ was shown to promote DNA repair in human glioblastoma cells (LN-Z308 and U251) and render them less susceptible to alkylating agent-mediated apoptosis (10). Together, these findings suggest that $p21^{WAF1/CIP1}$ protects cells from drug-mediated lethality through cell cycle- and/or DNA repair-related mechanisms.

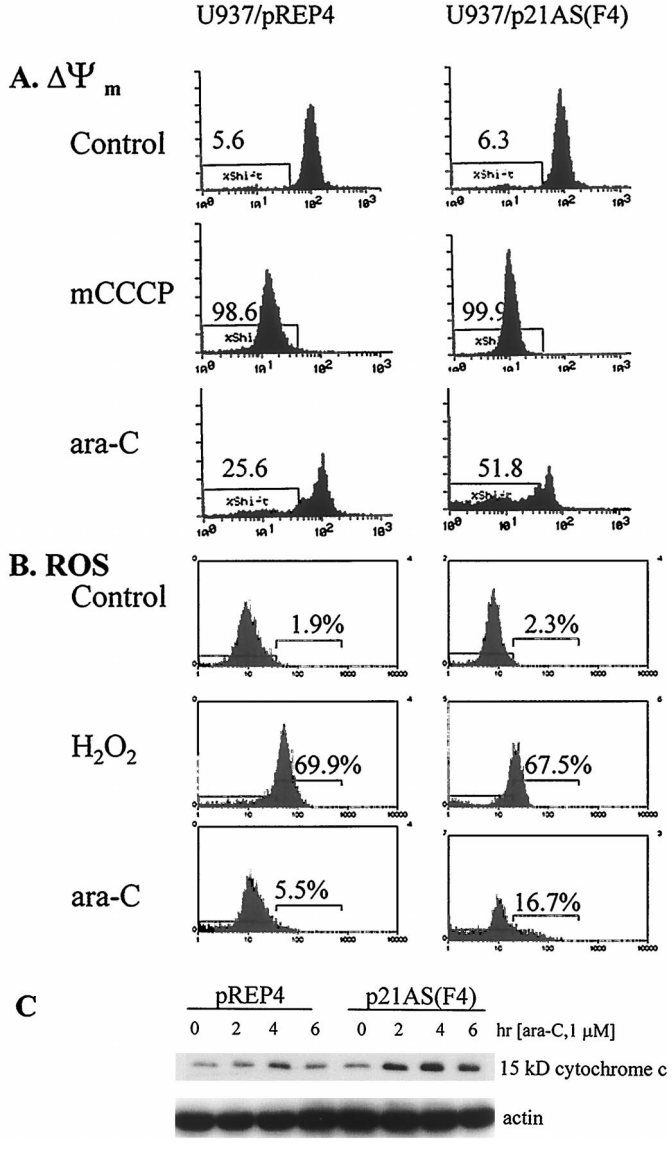

Fig. 6. *A*, after exposure of pREP 4 and p21AS/F4 cells to 1 μM ara-C for 6 h, $\Delta\psi_m$ was monitored by flow cytometry using $DiOC_6$ as a probe. Results obtained with the protonophore *m*-chlorophenylhydrazone (*mCCCP*), which causes complete collapse of the $\Delta\psi_m$, are shown for comparison. Values represent the percentage of cells exhibiting low $DiOC_6$ uptake; two additional studies yielded equivalent results. *B*, generation of ROS was monitored in cells treated as above by flow cytometry using DHR 123 as described in the text. Results obtained using H_2O_2 are shown for comparison. Values represent the percentage of cells exhibiting high DHR 123 fluorescence; two additional studies yielded equivalent results. *C*, after treatment as above, cytosolic S-100 fractions were isolated from pREP4 and p21AS/F4 cells, and expression of cytochrome *c* was assessed by Western blot analysis as described in the text. Actin controls are shown to document equal loading of lanes and protein transfer. Two additional studies yielded equivalent results.

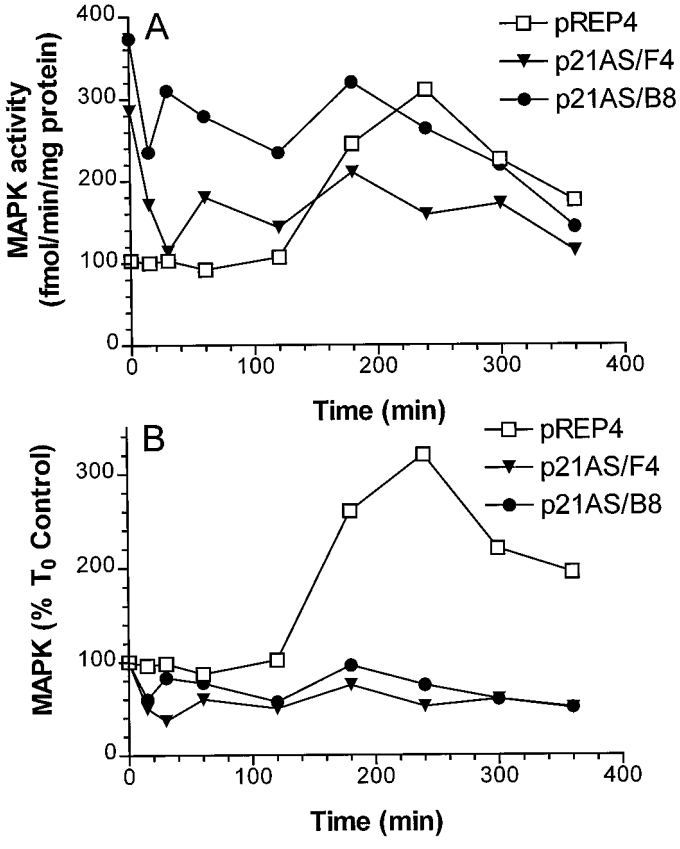

Fig. 7. *A*, logarithmically growing pREP4 (□), p21AS/F4 (▼), and p21AS/B8 (●) cells were exposed to 1 μM ara-C for 6 h, and at the designated intervals, MAP kinase activity, manifested by the phosphorylation of myelin basic protein, was determined as described in "Materials and Methods." Values, expressed as fmol [^{32}P]myelin basic protein/min/mg protein, represent the means for duplicate experiments. *B*, MAP kinase activity was monitored in ara-C-treated cells as described above and at each interval was expressed as a percentage relative to T_0 control values. In each case, variability between experiments was generally ≤15%.

Despite certain similarities, important differences exist between the present results and results reported previously. For example, in the study by Waldman *et al.* (8), enhanced apoptotic responses of p21$^{WAF1/CIP1}$-deficient cells to DNA-damaging agents were noted at relatively late time intervals (*e.g.*, at 30 h and most notably at 60–90 h after drug administration), which permitted cells to undergo at least one and in some cases more than one round of DNA synthesis. Analogously, in the study by Ruan *et al.* (10), p21$^{WAF1/CIP1}$-mediated protection from alkylator-induced apoptosis was noted 7 days after drug administration. In marked contrast, dysregulation of p21$^{WAF1/CIP1}$ in U937 cells rendered them dramatically more susceptible to ara-C-induced apoptosis within 4–6 h of drug exposure. In view of the relatively long generation time of leukemic blasts (*e.g.*, ≥ 30 h; 37), it is extremely unlikely that a shortened cell cycle traverse of p21 antisense-expressing cells could fully account for the early increase in drug susceptibility. Furthermore, partial synchronization of cells in S-phase by APH amplified the differential sensitivity of control and mutant cells to ara-C-induced cell death, indicating that dysregulation of p21$^{WAF1/CIP1}$ enhanced the intrinsic vulnerability of S-phase cells to ara-C actions. Although interference with DNA repair by p21$^{WAF1/CIP1}$ dysregulation cannot be ruled out, equivalent incorporation of ara-C residues into the DNA of mutant and control cells argues against this possibility. Collectively, these findings suggest that the mechanism by which p21$^{WAF1/CIP1}$ dysregulation renders U937 cells more sensitive to ara-C at early time points differs fundamentally from that involved in late-stage potentiation of apoptosis in colon tumor and glioblastoma cells treated with DNA-damaging agents (8–10).

Given evidence linking apoptosis to mitochondrial events (38, 39), it is tempting to relate increased ara-C susceptibility of p21$^{WAF1/CIP1}$ antisense-expressing cells to a lowered threshold for mitochondrial damage. Release of cytochrome *c* from mitochondria leads to the formation, in the presence of dATP, of a complex consisting of apoptosis-activating factor 1 (Apaf-1; the mammalian *Ced*-4 homologue) and caspase-9 (Apaf-3; 40), which, in turn, cleaves and activates caspase-3 (Yama; CPP32), thereby initiating the proteolytic apoptotic cascade. It is presently uncertain whether loss of mitochondrial membrane potential represents the central initiating event in apoptosis (17), given evidence that cytochrome *c* release may precede the collapse in $\Delta\psi_m$ (18, 41). On the other hand, the ability of certain agents to induce apoptosis in the absence of cytochrome *c* release (42, 43) suggests the existence of cytochrome *c*-independent cell death pathways. In the present study, the reduction in $\Delta\psi_m$ and release of cytochrome *c* accompanying ara-C treatment was more marked in p21-antisense cells as early as 2 h and most prominently at 4–6 h after drug exposure, although the close temporal relationship between these events makes it difficult to determine which was primarily responsible for enhanced lethality. Nevertheless, these findings indicate that dysregulation of p21$^{WAF1/CIP1}$ lowers the threshold for mitochondrial dysfunction after ara-C treatment. It is noteworthy that p21 antisense-expressing cells exposed to ara-C displayed a relatively modest enhancement in ROS generation, consistent with the notion that induction of ROS lags behind and represents a consequence of earlier mitochondrial damage (41). It is also important to note that the increased susceptibility of p21$^{WAF1/CIP1}$ antisense-expressing cells to ara-C-mediated mitochondrial dysfunction was accompanied by a loss in leukemic cell self-renewal capacity, particularly in view of reports suggesting a discordance between apoptosis and loss of clonogenic potential (27, 30, 44).

Although disruption of p21$^{WAF1/CIP1}$ function has been shown to increase the sensitivity of tumor cells to various agents (8–10), this has not been a universal finding. For example, antisense-mediated disruption of p21$^{WAF1/CIP1}$ reduced antioxidant-related apoptosis and potentiation of 5-FU-mediated lethality in human colon cancer cells (HCT 15 and HCT 116) in a p53-independent manner (45). However, interference with p21$^{WAF1/CIP1}$ function in HCT 116 cells did not directly alter 5-FU sensitivity. Enforced expression of p21$^{WAF1/CIP1}$ has also been shown to enhance apoptosis in pRb-negative osteosarcoma cells (SaOs-2) exposed to the antimetabolites methotrexate and tomudex, a phenomenon attributed to inhibition of E2F-1 phosphorylation and activity (46). The basis for divergent effects of p21$^{WAF1/CIP1}$ dysfunction on the drug sensitivity of myelomonocytic *versus* promyelocytic leukemia cells (15) is unclear but may stem from unique features of the HL-60 cell line, including amplification of c-*myc* (47). Together, these findings indicate that the net effect of p21$^{WAF1/CIP1}$ dysregulation on drug sensitivity depends upon the molecular context in which it occurs, as well as the inciting agent.

After ara-C treatment, p21 antisense-expressing cells displayed a more prominent high mobility, putatively dephosphorylated pRb species than their empty vector counterparts. The ability of ara-C to induce pRb dephosphorylation in HL-60 cells has been described previously (27). However, it has been shown recently that cleavage of pRb during apoptosis can generate a fragment that comigrates with the dephosphorylated pRb protein (48). Although the increase in abundance of such a fragment in p21 antisense-expressing cells could represent a consequence of enhanced susceptibility to ara-C-mediated cell death, results obtained with an antibody specific for underphosphorylated pRb (Fig. 4*B*) demonstrate that p21$^{WAF1/CIP1}$ dysregulation specifically promotes ara-C-associated pRb dephosphorylation. Lastly, the divergent effects of p21$^{WAF1/CIP1}$ dysregulation on PMA-induced (16) *versus* ara-C-induced underphosphorylation of pRb sug-

gest that these agents modify pRb phosphorylation status through different mechanisms.

Several lines of evidence, including demonstration of transcriptional activation of $p21^{WAF1/CIP1}$ expression through the MAP kinase signaling cascade (33), suggest a link between $p21^{WAF1/CIP1}$ induction and the ERK/MAP kinase survival pathway. Although $p21^{WAF1/CIP1}$ has been reported to inhibit activation of the stress-related JNK/SAPK cascade (34), $p21^{WAF1/CIP1}$ dysregulation failed to modify the JNK response to ara-C in the present study. In contrast, p21 antisense-expressing cells exhibited higher basal levels of MAP kinase activity than their pREP4 counterparts but did not exhibit increases in activity after ara-C exposure. MAP kinase has been linked to cell survival (32) and has also been implicated in cellular maturation (49), an event that under some circumstances opposes drug-induced apoptosis (50). Furthermore, stresses imposed by cytotoxic drugs such as ara-C are known to induce MAP kinase in leukemic cells (51), and agents that interrupt the MAP kinase cascade (*e.g.*, PD98059) potentiate apoptosis in cells exposed to H_2O_2 (52) as well as ara-C and Taxol (53, 54). It is therefore possible that attenuation of MAP kinase activation over basal levels in p21 antisense-expressing cells contributes to their enhanced susceptibility to ara-C-related apoptosis. An alternative possibility is that functional $p21^{WAF1/CIP1}$ may be required for MAP kinase-related cytoprotective actions.

In summary, the present studies demonstrate that dysregulation of the CDKI $p21^{WAF1/CIP1}$ increases the susceptibility of U937 myelomonocytic leukemia cells to ara-C-mediated apoptosis, a phenomenon that is associated with early alterations in mitochondrial function (*e.g.*, loss of $\Delta\psi_m$ and release of cytochrome *c* into the cytosol). Thus, in addition to disruption of cell cycle-related events (9) and interference with DNA repair (10), facilitation of mitochondrial damage represents an alternative means by which $p21^{WAF1/CIP1}$ dysregulation can promote drug-related apoptosis. The mechanism by which potentiation of mitochondrial damage occurs is unclear, although it is known that $p21^{WAF1/CIP1}$ forms a complex with cyclins, CDKs, and the DNA replication/repair-related proliferating cell nuclear antigen (55). It is possible that perturbations stemming from $p21^{WAF1/CIP1}$ dysregulation modify proliferating cell nuclear antigen activity, thereby amplifying DNA damage signals through an as yet unidentified pathway. Moreover, the results of a recent study suggest that the cell cycle checkpoint gene *p53* triggers early expression of a group of redox-related p53-inducible genes, activation of which is associated with mitochondrial degradation and ultimately, cell death (56). Because $p21^{WAF1/CIP1}$ represents a major downstream effector of p53 (5) and is also induced in p53-null cells (6, 7), the notion that $p21^{WAF1/CIP1}$ might be involved in the regulation of such redox-associated p53-inducible genes appears plausible. Further studies involving $p21^{WAF1/CIP1}$ may yield important information concerning novel molecular determinants of ara-C sensitivity in leukemia, and could also provide mechanistic insights into interactions between cytotoxic drugs and differentiation-inducing agents known to trigger CDKI expression.

REFERENCES

1. Elledge, S. J., and Harper, J. W. Cdk inhibitors: on the threshold of checkpoints and development. Curr. Opin. Cell Biol., *6:* 847–852, 1994.
2. Chellapan, S., Giordanao, A., and Fisher, P. B. The role of cyclin-dependent kinases and their inhibitors in cellular differentiation and development. Curr. Topics Microbiol. Immunol., *227:* 57–103, 1998.
3. Morgan, D. O. Principles of cdk regulation. Nature (Lond.), *374:* 131–134, 1995.
4. Harper, J. W., Adami, G. R., Wei, N., Heyomarsi, K., and Elledge, S. J. The p21 Cdk-interacting protein Cip1 is a potent inhibitor of G1 cyclin-dependent kinases. Cell, *75:* 805–816, 1993.
5. El-Diery, W. S., Harper, J. W., O'Connor, P. M., Velculescu, V. E., Canman, C. E., Jackman, J., Pietenpol, J. A., Burrell, M., Hill, D. E., Wang, Y., Wiman, K. G., Mercer, W. E., Kastan, M. B., Hohn, K. W., Elledge, S. J., Kinzler, K. W., and Vogelstein, B. WAF1/CIP1 is induced in p53-mediated G_1 arrest and apoptosis. Cancer Res., *54:* 1169–1174, 1994.
6. Jiang, H., Lin, J., Su, Z-Z., Collart, F. R., Huberman, E., and Fisher, P. B. Induction of differentiation in human promyelocytic leukemia cells activates p21, WAF1/CIP1, expression in the absence of p53. Oncogene, *9:* 3397–3406, 1994.
7. Steinman, R. A., Hoffman, B., Iro, A., Guillof, C., Liebermann, D. A., and El-Housseni, E. M. Induction of *p21* (WAF-1/CIP1) during differentiation. Oncogene, *9:* 3389–3396, 1994.
8. Waldman, T., Lengauer, C., Kinzler, K. W., and Vogelstein, B. Uncoupling of S phase and mitosis induced by anticancer agents in cells lacking p21. Nature (Lond.), *381:* 713–716, 1996.
9. Waldman, T., Zhang, Y., Dellehay, L., Yu, J., Kinzler, K., Vogelstein, B., and Williams, J. Cell-cycle arrest *versus* cell death in cancer therapy. Nat. Med., *3:* 1034–1036, 1997.
10. Ruan, S., Okcu, M. F., Ren, J. P., Chiao, P., Andreef, M., Levin, V., and Zhang, W. Overexpressed WAF1/Cip1 renders glioblastoma cells resistant to chemotherapy agents 1,3-bis(2-chloroethyl)-1-nitrosourea and cisplatin. Cancer Res., *58:* 1538–1543, 1998.
11. St. Croix, B., Florenes, V. A., Rak, J. W., Flanagan, M., Bhattacharya, N., Slingerland, J. M., and Kerbel, R. S. Impact of the cyclin-dependent kinase inhibitor $p27^{Kip1}$ on resistance of tumor cells to anticancer agents. Nat. Med., *2:* 1204–1210, 1996.
12. Stone, S., Dayananth, P., and Kamb, A. Reversible, p16-mediated cell cycle arrest as protection from chemotherapy. Cancer Res., *56:* 3199–3202, 1996.
13. McDonald, E. R., Wu, G. S., Waldman, T., El-Diery, W. S. Repair defect in $p21^{WAF1/CIP1}$ −/− human cancer cells. Cancer Res., *56:* 2250–2255, 1996.
14. Gunji, H., Kharbanda, S., and Kufe, D. Induction of internucleosomal DNA fragmentation in human myeloid leukemia cells by 1-β-D-arabinofuranosylcytosine. Cancer Res., *51:* 71–74, 1991.
15. Freemerman, A. J., Vrana, J., Tombes, R. M., Jiang, H., Chellepan, S. P., Fisher, P. B., and Grant, S. Effects of antisense p21 (WAF1/CIPI//MDA6) expression on the responses of human myeloid leukemia cells to differentiation inducing and cytotoxic agents. Leukemia (Baltimore), *11:* 504–513, 1997.
16. Wang, Z., Su, Z-Z., Fisher, P. B., Van Tuyle, G., and Grant, S. Reciprocal regulation of PKC activator-induced apoptosis and differentiation in human leukemia cells by the cyclin-dependent kinase inhibitor $p21^{WAF1/CIP1/MDA6}$. Exp. Cell Res., *244:* 105–116, 1998.
17. Marchetti, P., Casteldo, M., Susin, S. A., Zamzami, N., Hirsch, T., Macho, A., Haeffner, A., Hirsch, F., Geuskens, M., and Kroemer, G. Mitochondrial permeability transition is a central coordinating event of apoptosis. J. Exp. Med., *184:* 1155–1160, 1996.
18. Yang, J., Liu, X., Bhalla, K., Kim, C. N., Ibrado, A. M., Cai, J., Peng, T-I., Jones, D. P., and Wang, X. Prevention of apoptosis by Bcl-2: release of cytochrome c from mitochondria blocked. Science (Washington DC), *275:* 1129–1132, 1997.
19. Sundstrom, C., and Nilsson, K., Establishment and characterization of a human histiocytic lymphoma cell line (U937). Int. J. Cancer, *17:* 565–577, 1976.
20. Jarvis, W. D., Gewirtz, D. A., Povirk, L., Turner, A., Traylor, R., Pettit, G. R., and Grant, S. Effect of bryostatin 1 and other activators of protein kinase C on 1-β-D-arabinofuranosylcytosine-induced apoptosis in HL-60 human promyelocytic leukemia cells. Biochem. Pharmacol., *47:* 839–852, 1994.
21. Bhalla, K., MacLaughlin, W., Cole, J., Arlin, Z., Baker, M., Graham, G., and Grant, S. Deoxycytidine preferentially protects normal *versus* leukemic myeloid progenitor cells from cytosine arabinoside-mediated cytotoxicity. Blood, *2:* 568–571, 1987.
22. Frey, T. Correlated flow cytometric analysis of terminal events in apoptosis reveals the absence of some changes in some model systems. Cytometry, *28:* 253–263, 1997.
23. Jarvis, W. D., Fornari, F. A., Auer, K. L., Freemerman, A. J., Szabo, E., Birrer, M. J., Barbour, S. E., Dent, P., and Grant, S. Differential involvement of stress-activated and mitogen-activated protein kinases in the apoptotic actions of ceramide and sphingosine. Mol. Pharmacol., *52:* 935–947, 1997.
24. Oltvai, Z. N., Milliman, C. L., and Korsmeyer, S. J. Bcl-2 heterodimerizes *in vivo* with a conserved homolog, Bax, that accelerates programmed cell death. Cell, *74:* 609–619, 1993.
25. Major, P., Egan, E. M., Beardsley, G. P., Minden, M. D., and Kufe, D. W. Lethality of human myeloblasts correlates with incorporation of ara-C into DNA. Proc. Natl. Acad. Sci. USA, *78:* 3235–3229, 1981.
26. Young, R. S. K., and Fischer, G. A. The action of arabinofuranosylcytosine on synchronously growing populations of mammalian cells. Biochem. Biophys. Res. Commun., *32:* 23–29, 1968.
27. Dou, Q. P., and Lui, V. W. Y. Failure to dephosphorylate retinoblastoma protein in drug-resistant cells. Cancer Res., *55:* 5222–5225, 1995.
28. Dunaef, J. L., Stober, B. E., Guha, S., Khavari, P. A., Alin, K., Luban, J., Begemann, M., Brabtree, G. R., and Goff, S. P. The retinoblastoma protein and BRG1 form a complex and cooperate to induce cell cycle arrest. Cell, *79:* 119–130, 1994.
29. Yin, D. X., and Schimke, R. T. Bcl-2 expression delays drug-induced apoptosis but does not increase clonogenic survival after drug treatment in HeLa cells. Cancer Res., *55:* 4922–4928, 1995.
30. Brunet, C. L., Gunby, R. H., Benson, S. P. R., Hickman, J. A., Watson, A. J. M., and Brady, G. Commitment to cell death measured by loss of clonogenicity is separable from the appearance of apoptotic markers. Cell Death Differ., *5:* 107–115, 1998.
31. Ikegami, S., Taguchi, T., Ohashi, M., Oguro, M., Nagano, H., and Mano, Y. Aphidicolin prevents mitotic cell division by interfering with the activity of DNA polymerase-α. Nature (Lond.), *275:* 458–460, 1978.
32. Xia, Z., Dickens, M., Raingeaud, J., Davis, R. J., Greenberg, M. E. Opposing effects of ERK and JNK-p38 MAP kinases on apoptosis. Science (Washington DC), *270:* 1326–1331, 1995.

33. Liu, Y., Martindale, J. L., Gorospe, M., and Holbrook, N. J. Regulation of $p21^{WAF1/CIP1}$ expression through mitogen-activated protein kinase signaling pathway. Cancer Res., *56:* 31–35, 1996.
34. Shim, J., Lee, H., Park, J., Kim, H., and Choi, E-J. A non-enzymatic p21 protein inhibitor of stress-activated protein kinases. Nature (Lond.), *381:* 804–807, 1996.
35. Jiang, H., and Fisher, P. B. Use of an efficient subtraction hybridization protocol for the identification of genes differentially regulated during the induction of differentiation in human melanoma cells. Mol. Cell. Differ., *1:* 285–299, 1993.
36. Wang, J., and Walsh, K. Resistance to apoptosis conferred by Cdk inhibitors during myocyte differentiation. Science (Washington DC), *273:* 359–361, 1996.
37. Greenberg, M. L., Chanana, A. D., Cronkite, E. P., Giacomelli, G., Schiffer, L. M., Stryctmans, P. A., and Vincent, P. C. The generation time of human leukemic myeloblasts. Lab. Invest., *26:* 245–252, 1972.
38. Kim, C. N., Wang, X., Huang, Y., Ibrado, A. M., Liu, L., Fang, G., and Bhalla, K. Overexpression of Bcl-xL inhibits ara-C-induced mitochondrial loss of cytochrome c and other perturbations that activate the molecular cascade of apoptosis. Cancer Res., *57:* 3115–3120, 1997.
39. Backway, K. L., McCulloch, E. A., Chow, S., and Hedley, D. W. Relationship between the mitochondrial permeability transition and oxidative stress during ara-C toxicity. Cancer Res., *37:* 2446–2451, 1997.
40. Li, P., Nijhawan, D., Budihardjo, I., Srinivasula, S. M., Ahmad, M., Alnemri, E. S., and Wang, X. Cytochrome c and dATP-dependent formation of Apaf-1/caspase-9 complex initiates an apoptotic protease cascade. Cell, *91:* 479–489, 1997.
41. Bossy-Wetzel, E., Newmeyer, D. D., and Green, D. R. Mitochondrial cytochrome c release in apoptosis occurs upstream of DEVD-specific caspase activation and independently of mitochondrial transmembrane depolarization. EMBO J., *17:* 37–49, 1998.
42. Chauhan, D., Pandey, P., Ogata, A., Teoh, G., Krett, N., Halgren, R., Rosen, S., Kufe, D., Kharbanda, S., and Anderson, K. Cytochrome c-dependent and -independent induction of apoptosis in multiple myeloma cells. J. Biol. Chem., *272:* 29995–29997, 1997.
43. Tang, D. G., Li, L., Zhu, Z., and Joshi, B. Apoptosis in the absence of cytochrome c accumulation in the cytosol. Biochem. Biophys. Res. Commun., *242:* 380–384, 1998.
44. McCarthy, N. J., Whyte, M. K. B., Gilbert, C. S., and Evan, G. I. Inhibition by Ced-3/ICE-related proteases does not prevent cell death induced by oncogenes, DNA damage, or the Bcl-2 homolog Bak. J. Cell Biol., *136:* 215–227, 1997.
45. Chinery, R., Brockman, J. A., Peeler, M. O., Shyr, Y., Beauchamp, R. D., and Coffey, R. J. Antioxidants enhance the cytotoxicity of chemotherapeutic agents in colorectal cancer: a p53-indenpendent induction of $p21^{WAF1/CIP1}$ via C/EBPβ. Nat. Med., *3:* 1233–1241, 1997.
46. Li, W., Fan, J., Hochhauser, D., and Bertino, J. R. Overexpression of $p21^{WAF1}$ leads to increased inhibition of E2F-1 phosphorylation and sensitivity to anticancer drugs in retinoblastoma-negative human sarcoma cells. Cancer Res., *57:* 2193–2199, 1997.
47. Collins, S., and Groudine, M. Amplification of endogenous *myc*-related DNA sequences in a human myeloid leukemia cell line. Nature (Lond.), *298:* 679–681, 1982.
48. Chen, W-D., Otterson, G. A., Lipkowitz, S., Khleif, S. N., Coxon, A. B., and Kaye, F. J. Apoptosis is associated with cleavage of a 5 kDa fragment from RB which mimics dephosphorylation and modulates E2F binding. Oncogene, *14:* 1243–1248, 1997.
49. Kharbanda, S., Saleem, A., Emoto, Y., Stone, R., Rapp, U., and Kufe, D. Activation of Raf-1 and mitogen-activated protein kinases during monocytic differentiation of human myeloid leukemia cells. J. Biol. Chem., *269:* 872–878, 1994.
50. Solary, E., Bertrand, R., Kohn, K. W., and Pommier, Y. Differential induction of apoptosis in undifferentiated and differentiated HL-60 cells by DNA topoisomerase I and II inhibitors. Blood, *81:* 1359–1368, 1993.
51. Kharbanda, S., Emoto, Y., Kisaki, H., Saleem, A., and Kufe, D. 1-β-D-Arabinofuranosylcytosine activates serine/threonine kinases and c-*jun* gene expression in phorbol ester-resistant myeloid leukemia cells. Mol. Pharmacol., *46:* 67–72, 1994.
52. Wang, X., Martindale, J. L., Liu, Y., and Holbrook, N. J. The cellular response to oxidative stress: influence of mitogen-activated protein kinase signalling pathways on cell survival. Biochem. J., *333:* 291–300, 1998.
53. Jarvis, W. D., Fornari, F. A., Tombes, R. M., Martin, H. A., Erkulla, R. K., Bittman, R., Schwartz, G. K., Dent, P., and Grant, S. Evidence for involvement of MAPK, rather than SAPK, in potentiation of 1-β-D-arabinofuranosylcytosine-induced apoptosis by interruption of the PKC pathway. Mol. Pharmacol., *54:* 844–856, 1998.
54. Wang, S., Guo, Y., Castillo, T., Dent, P., and Grant, S. Potentiation of Taxol-induced apoptosis and antiproliferative effects in human myeloid leukemia cells (U937) by bryostatin 1. Biochem. Pharmacol., *56:* 635–644, 1998.
55. Waga, S., Hannon, G. J., Beach, D., and Stillman, B. The p21 inhibitor of cyclin-dependent kinases controls DNA replication through interaction with PCNA. Nature (Lond.), *369:* 574–578, 1994.
56. Polyak, K., Xia, Y., Zweier, J. L., Kinzler, K. W., and Vogelstein, B. A model for p53-induced apoptosis. Nature (Lond.), *369:* 300–305, 1997.